



Published in final edited form as:

DNA Repair (Amst). 2019 December ; 84: 102614. doi:10.1016/j.dnarep.2019.04.002.

Genome Instability Consequences of RNase H2 Aicardi-Goutières Syndrome Alleles

Catherine J Potenski^{a,1}, Anastasiya Epshtein^a, Christopher Bianco^b, Hannah L. Klein^a

^aDepartment of Biochemistry and Molecular Pharmacology, New York University School of Medicine, New York, NY 10016, USA

^bDepartment of Microbiology, New York University School of Medicine, New York, NY 10016, USA

Abstract

The RNase H2 complex is a conserved heterotrimeric enzyme that degrades RNA:DNA hybrids and promotes excision of rNMPs misincorporated during DNA replication. Failure to remove ribonucleotides from DNA leads to genomic instability in yeast and humans. The monogenic Aicardi-Goutières syndrome (AGS) results from mutation in one of several genes, among which are those encoding the RNase H2 subunits. The complete cellular and genomic consequences of *RNASEH2* mutations and the precise connection to disease remain unclear. To learn more about the effect of *RNASEH2* mutations on the cell, we used yeast as a model of AGS disease. We have generated yeast strains bearing AGS-associated mutations in *RNASEH2* genes. There is a range of disease presentation in patients bearing these *RNASEH2* variants. Here we report on *in vivo* phenotypes of genomic instability, including mutation and recombination rates, and synthetic gene interactions. These phenotypes provide insight into molecular consequences of *RNASEH2* mutations, and lay the groundwork for further study of genomic instability as a contributing factor to AGS disease.

Keywords

Ribonucleotides; AGS; genome instability; recombination; mutagenesis; DNA replication

1. Introduction

Aicardi-Goutières syndrome is a recessive encephalopathy that affects the brain and immune system [1, 2]. Although affected children are born with features suggestive of a chronic prenatal viral infection [3], instead they carry mutations in one of six genes that result in an

Corresponding author: Hannah L. Klein, Department of Biochemistry and Molecular Pharmacology, New York University School of Medicine, New York, NY 10016, USA, hannah.klein@nyumc.org.

¹Current address: Nature Publishing Group, New York, NY 10004, USA

Conflicts of interest

The authors declare no conflicts of interest.

Publisher's Disclaimer: This is a PDF file of an unedited manuscript that has been accepted for publication. As a service to our customers we are providing this early version of the manuscript. The manuscript will undergo copyediting, typesetting, and review of the resulting proof before it is published in its final citable form. Please note that during the production process errors may be discovered which could affect the content, and all legal disclaimers that apply to the journal pertain.

undetermined defect in processing nucleic acids and an immune response against some nucleic acid product.

1.1 RNase H2 mutations in Aicardi-Goutières syndrome patients

RNASE H2 is a conserved enzyme complex that functions in DNA replication to eliminate rNMP residues that have been incorporated into DNA and additionally can remove longer RNA:DNA hybrids or R-loops [4]. Misincorporated ribonucleotides arise either through defects in Okazaki fragment processing or as a natural consequence of errors of replicative DNA polymerases [5, 6]. Misincorporated rNMPs that are not removed distort the DNA helix and cause replication stalling in the next replication cycle. Longer RNA:DNA hybrids may arise from incomplete processing of Okazaki fragment primers or from stalled transcription complexes [4, 7].

An extensive catalog of mutations in genes leading to AGS has shown that over 50% of the studied AGS families had mutations in the *RNASEH2A*, *RNASEH2B* or *RNASEH2C* genes [2, 8]. Of these, two-thirds occurred in the *RNASEH2B* gene. Most families carried biallelic mutations, often as compound heterozygotes, with the majority of the RNASE H2 mutations occurring in the *RNASEH2B* gene.

1.2 DNA damage events in RNase H2-defective yeast cells

In contrast to mouse systems [5, 9], the RNASE H2 genes of yeast, *RNH201*, *RNH202*, and *RNH203*, are not essential, making it possible to study the DNA damage consequences of embedded ribonucleotide residues in DNA. RNase H2 null allele mutants of yeast have phenotypes associated with DNA damage and genome instability, the most common being increased mutagenesis, increased recombination, increased loss of heterozygosity (LOH), increased chromosome loss and chromosome rearrangements.

Mutational events increased in RNase H2 null mutants of yeast have a particular signature, that of slippage in simple repeats [6, 10]. These mutations are seen only in the absence of functional RNase H2 activity and require the action of Topoisomerase I (Top1) [10, 11]. Yeast RNase H2 mutants also display a hyperrecombination phenotype [12]. The hyperrecombination phenotype was not dependent on the action of Top1 and was stimulated by tandem rNMP residues in DNA, in contrast to single rNMP residues being responsible for slippage mutagenesis [13, 14]. RNase H2 mutants isolated in a different study were also found to have a hyper-recombination phenotype [15].

1.3 Studies of human AGS mutations in human and mouse cells and biochemical activity of the RNASE H2 enzyme

Identification of mutations in the *RNASEH2A*, *RNASEH2B* and *RNASEH2C* genes among 127 families presenting with AGS revealed 73 pedigrees with mutations [2, 16]. Among the mutations observed was a homozygous mutation in *RNASEH2A* (c.109G>A, p.Gly37Ser) (“c” refers to the coding sequence or base which is altered and “p” refers to the amino acid residue which is altered, according to the standard nomenclature for human sequence variants [17]), predicted to affect catalytic activity, and a common mutation in *RNASEH2B* (c.529G>A, p.Ala177Thr), which occurred as homozygous and compound heterozygous in

patients [2], Enzymatic studies confirmed that the RNASEH2A-G37S protein had reduced activity [16], Modeling this mutation into the *Saccharomyces cerevisiae* Rnh201 protein (Rnh201-G42S) confirmed conservation of this mutation on biochemical activity [18], Modeling other AGS alleles on the *Saccharomyces cerevisiae* protein were unsuccessful in that no effect on enzymatic activity in vitro could be obtained [18, 19], Of note was the *rnh202-L52R* allele and associated protein, which we have studied through genetic means and is described below.

A more complete understanding of the effect of AGS RNASE H2 mutations on protein function became apparent after the structure of the human RNase H2 complex was solved [20]. Mapping of 29 human AGS mutations onto the crystal structure of the complex led to predictions of effects of these mutations on complex stability and substrate cleavage. Importantly, many AGS mutations mapped to the interface between the RNase H2 subunits and would affect stability of the heterotrimer but cleavage of a rNMP containing substrate in vitro would not be affected [21], accounting for the apparent normal activity in vitro of mutant proteins. The yeast system provides the opportunity to examine the DNA damage consequences of AGS hypomorphic alleles and thereby provide support for the link between DNA damage and autoimmunity arising from nonnull RNase H2 gene mutations.

2. Materials and Methods

2.1 Yeast growth conditions

All experiments were performed by growing yeast at 30°C in either rich medium (YPD) or synthetic media plus/minus amino acids or drugs.

2.2 Plasmid and yeast strain construction

All yeast strains are derivatives of W303. Strains are listed in Supplementary Table 1. To construct AGS yeast mutants, a portion of *RNH201* (−499-688) was PCR-amplified and cloned into YIplac211 integration plasmid using PstI and BamHI sites. A sequence encompassing the *RNH202* locus [−388-(+)786] was PCR-amplified and cloned into YIplac211 integration plasmid using SacI and PstI sites. Site-directed mutagenesis (QuikChange, Stratagene) was performed using the following oligos: *rnh201-G42S*: 5'-TCGATGAAGCTAGCAGAGGGCCCGT-3' and 5'-ACGGGCCCTCTGCTAGCTTCATCGA-3'; *rnh202-L52R*: 5'-GAAAATATTAATGGAAAACGTTACGAAATAAGATC-3' and 5'-GATCTTATTTTCGTAACGTTTTCCATTAATATTTT-3'; *rnh202-H109R*: 5'-CTCAAGCAAATACGCTTTTGTCTTTTATACG-3' and 5'-CGTATAAAGAACAAGCGTATTTTGCTTGAG-3'; *rnh202-L186F*: 5'-GTCGTCTCAAGAGTGGCTTTGCAAAAGTTAGTG-3' and 5'-CACTAACTTTTGCAAAGCCACTCTTGAGACGAC-3'; *rnh202-T204I*: 5'-CGTCTATTACAAGATCATATCTGCAATGATAACAC-3' and 5'-GTGTTATCATTGCAGATATGATCTTGTAATAGACG-5'.

Mutations were confirmed by sequencing. Plasmids were linearized to transform into yeast and integrants were selected on Sc-uracil. Transformants were patched to YPD and grown

overnight in YPD prior to plating on 5'FOA. FOA-resistant segregants were screened for presence of the mutation by sequencing the entire gene with some upstream and downstream regions included.

2.3 Recombination rate assay

Recombination rates were performed using the *leu2-ecoRI::URA3::leu2-bstEII* system as described [12]. At least 18 independent cultures with a minimum of two isolates per genotype were used to determine rates and 95% confidence limits [22].

2.4 Mutation rate assay

Mutation rates for the (AG)₄ slippage reporter and were determined by the Lea and Coulson median method [23] as previously described [10,11, 22].

2.5 Alkaline gel electrophoresis and quantification of ribonucleotide density

Alkaline gel analysis was performed as described [6]. Genomic DNA was isolated from yeast cells grown overnight in YPD using the MasterPure Yeast DNA isolation kit (Epicentre) according to the manufacturer's instructions. For alkaline treatment, ~10 µg purified DNA was incubated in 0.3M KOH for 2 hours at 55°C. Samples were mixed with 6X alkaline loading buffer (300 mM KOH, 6 mM EDTA, 18% Ficoll type 400, 0.15% bromocresol green, 0.25% xylene cyanol) and loaded onto a 1% agarose gel made with alkaline buffer (50 mM NaOH, 1 mM EDTA). Gels were run in 1X alkaline buffer (5 mM NaOH, 1 mM EDTA) for 18 h at 1 V/cm. Gels were neutralized by gently shaking in neutralizing buffer (1 M Tris-HCl, 1.5 M NaCl, pH 7.5) for 1 h and stained with 0.5 µg/mL ethidium bromide for 30 min, followed by destaining for 15 min in dH₂O. For neutral gels, ~2 µg purified DNA was run on 1% agarose gel 1 X TBE. Staining procedures were the same as for the alkaline gels, minus the neutralization step.

Extraction and quantification of gel data intensity profiles was carried out using Matlab code. The intensity profile (as a function of gel length) for each lane was calculated by averaging over the width of the lane followed by background subtraction. To obtain the background profile subtraction, the background profile was obtained by averaging the gap spacing on both sides of each lane. The Y-axis scale (in kb) was determined by extrapolating the specific peaks location of the different DNA fragments obtained in the intensity profile of the DNA ladder band, and this kb scale transformed onto the Y-axis of the lane profiles. The maximum of each peak was normalized to 1 and the X-axis scale are arbitrary labels to 1.

3. Results

3.1 Identification of conserved AGS-associated residues in yeast RNase H2 subunits

To create structural models of yeast RNaseH2 proteins, translated sequences of *RNH202* and *RNH201* obtained from the *Saccharomyces* Genome Database were submitted to the protein structure prediction server I-TASSER [24]. The resultant homology models were aligned to human RNaseH2 protein structures (PDB ID = 3PUF [20] using the COFACTOR server [25]. Images of aligned models were generated using PyMOL (Figure 1A, B). The aligned

structural models were used to identify yeast residues equivalent to human residues mutated in AGS patients [2, 16]. From human RNaseH2A, residue Gly37 aligned to yeast Rnh201 residue Gly42 (Figure 1A). From human RNaseH2B, the following residues aligned to yeast Rnh202: hLeu60 to yLeu52; hHis86 to yH109; hLeu138 to yLeu186; and hSer159 to yThr204 (Figure 1B). These residues were found in various parts of the RNase H2 complex (Figure 1C). The alignments were also seen using Clustal Omega (Figure 1D). RNaseH2A is the catalytic subunit of the enzyme, and the exact functions of RNaseH2B and RNaseH2C still remain unclear, although these subunits are needed for the catalytic activity of RNaseH2A to be functional and are suggested to provide structural support as well as protein interaction platform [19]. We constructed yeast mutants bearing the same amino acid change that was seen clinically (Figure 1E), generating 5 AGS mutant strains: *rnh201-G42S*, *rnh202-L52R*, *rnh202-H109R*, *rnh202-L186F* and *rnh202-T204I*, and assayed these AGS strains for genome instability.

3.2 Yeast AGS allele gene interactions

Deletions of any of the three RNaseH2 genes are synthetically sick/lethal with a known list of gene deletions that compromise genes involved in replication and DNA damage repair, including the genes of the MRX complex (*MRE11*, *RAD50* and *XRS2*) [11]. We crossed the AGS mutant strains to a *rad50* strain, sporulated and dissected tetrads.

Two mutants, *rnh201-G42S* and *rnh202-L52R*, showed synthetic sickness with *rad50A* to a degree similar to that of a *rnh202* null mutant (Figure 2A). The other three mutants, *rnh202-H109R*, *rnh202-L186F* and *rnh202-T204I*, did not display any synthetic sickness with the *rad50* strain (Figure 2A). This recapitulates the *in vitro* data for the *rnh201-G42S* protein, which was shown to have reduced activity [18]. However, the result with the *rnh202-L52R* mutant was opposite from the *in vitro* data, as it had been shown to have wild type activity [18].

We examined the interaction with deletions of both *RNH1* (encoding RNase H1) and *TOP1* (encoding Topoisomerase I) as the triple mutant *rnh1 rnh2 top1* is lethal [26]. In contrast to the growth defect seen with a *rad50* mutation, only null alleles *rnh201* and *rnh202* plus *rnh202-L52R* had a synthetic growth defect (Figure 2B). This indicates that the RNase H2 activity remaining in *rnh201-G42S* is sufficient to buffer against loss of RNase H1 and Top1 activities, as initially described [13]. It suggests that activity of the RNase H2 complex with the *rnh202-L52R* subunit is below that of the complex with the *rnh201-G42S* subunit. The structure of the human RNase H2 complex predicts that the *rnaseh2B-L60R* subunit impairs stability of the complex [20].

3.3 Yeast AGS alleles and genome instability assays

We used intrachromosomal gene conversion and mutation of a slippage repeat reporter to examine the impact of AGS alleles on genome stability. In accordance with the synthetic sickness data, *rnh201-G42S* and the *rnh202-L52R* mutants showed an increase in recombination rate, although the level was not as high as the null mutant (Figure 3A). Nonetheless, the increase in recombination in the *rnh202-L52R* mutant approached that of the null allele and was significantly higher than the *rnh201-G42S* mutant, indicating a strong

loss of RNase H2 function. The *rnh202-H109R*, *rnh202-L186F* and *rnh202-T204I* mutants had recombination levels similar to those of wild type cells (Figure 3A).

We evaluated the mutation using a reporter system that assays specifically for slippages in an (AG)₄ repeat sequence [10, 27] as RNase H2 null alleles have a 100X increase in mutation rate, giving a wide range for assessment of hypomorphic mutations. The *rnh201-G42S* mutant had a significant increase in the dinucleotide slippage rate that was approximately the same fractional increase compared to the null allele rate as that seen for the recombination rate (Figure 3B). Similarly, the mutation slippage rate for the *rnh202-L52R* mutant was greatly increased, to close to the same fractional increase for the recombination rate (Figure 3B). The greater impact of the *rnh202-L52R* mutation on genome stability is also in accord with the synthetic lethal growth phenotype with *rnh1 top1*. As expected, the *rnh202-H109R*, *rnh202-L186F* and *rnh202-T204I* mutant strains had dinucleotide slippage rates similar to those of wildtype (Figure 3B).

3.4 Yeast AGS alleles and ribonucleotides in DNA

Genomic ribonucleotides can be detected by fragmentation on alkaline gels after alkaline treatment. Deletion of *RNH201* or *RNH202* results in a marked increase in smearing of DNA on alkaline gels, indicating more ribonucleotides embedded in these genomes (Figure 4). There are no detectable differences on neutral gels. Densitometric tracings of the alkaline gels shows increased fragmentation in the genomic DNA of the *rnh201-G42S* and *rnh202-L52R* strains and this is confirmed by determining the fraction of total DNA fragments migrating between 3 kb and 5 kb. Both null strains *rnh201* and *rnh202* show an increase in this fraction compared to wildtype following alkaline treatment. In contrast, genomic DNAs from the *rnh202-H109R*, *rnh202-L186F*, and *rnh202-T204I* strains showed no discernable changes in migration compared to *RNH202* following alkaline treatment. These results suggest reduced RNase H2 activity in these mutant strains, which most likely accounts for the increased mutation and recombination rates and synthetic phenotypes with *rad50* and *rnh1 top1* mutations.

4. Discussion and conclusions

The allele *rnh201-G42S* in the *RNASEH2A/RNH201* gene encodes a variant protein that is significantly reduced in enzymatic activity [16, 18, 19]. Our assays for genome instability and DNA migration on alkaline gels show that the *rnh201-G42S* mutant has some phenotypes indistinguishable from the null allele but others that lie between wildtype and the null allele. Previous studies showed that the *rnh201-G42S* allele has a mutational profile of the *CAN1* gene that is altered from the wildtype allele but is not as strong as the *rnh201* null allele [13]. Alkaline gel analysis suggested a slight increase in fragment mobility of DNA from the *rnh201-G42S* strain. In contrast, the *rnh201-G42S rnh1 top1* strain gave good growth that was barely distinguishable from wildtype, as initially shown [13], perhaps indicating that the residual activity is sufficient for removal of R-loops. This modest effect in yeast should be considered in contrast to the phenotype seen in mouse where the *Rnaseh2A-G37S* mutation is a perinatal lethal [28]. The *RNH202* alleles studied here occur as compound heterozygotes in AGS patients and frequently the other allele is *RNASEH2B* (c.

529G>A, p.Ala177Thr) [2, 16]. We observed a range of phenotypes among the *rnh202* strains that we generated. The fact that the mutations give rise to AGS when the other allele is *RNASEH2B* (c.529G>A, p.Ala177Thr) suggests that there is some impairment of the protein function in the compound heterozygous state. As the human genome is approximately 100-fold the size of the *S. cerevisiae* genome, with approximately 100-fold more rNMP residues incorporated into the genome every replication cycle [6, 9, 29], hypomorphic *RNASEH2B* mutations may have a phenotypic consequence in humans not observable in *S. cerevisiae*. Some mutant AGS proteins have normal activity against single rNMP residues in DNA but are defective against R-loops, another substrate for the RNase H2 activity.

In contrast, the *mh202-L52R/RNASEH2B* (c.179T>G, p.Leu60Arg) allele showed significant defects in all assays, suggesting that rNMP residues are not efficiently removed by the mutant RNase H2 protein and further processing contributes to genome instability and DNA damage. However, the *S. cerevisiae* RNase H2 protein with the Rnh202L52R subunit has 74% of wildtype activity in vitro [18]. The mutant RNase H2 complex could be more unstable in vivo or in lower amounts, or affected in recruitment to rNMP substrates in vivo. Whether the AGS phenotypes are more severe in patients with this allele and whether this contributes to the disease presentation is not known.

The discordance between the in vitro biochemistry and the in vivo yeast phenotypes and disease presentation in humans remains a challenge to understand the causes of AGS disease. The cGAS/STING pathway is stimulated by DNA damage [30, 31] and RNase H2 AGS mutations can stimulate the cGAS/STING pathway [28, 32]. Still, a direct link between DNA damage, genome instability and AGS presentation is not proven. The DNA damage sensor MRE11, which interacts with RAD50, is conserved between *S. cerevisiae* and humans and in human cells it is linked to the cGAS/STING pathway through recognition of cytosolic double-stranded DNA [33]. Recent studies on Topoisomerase I acting at rNMPs in DNA have shown that double strand breaks can be formed [34], and these could be the initiating substrate for homologous recombination. As RNase H2 has two activities, one against single rNMP residues in DNA and the second against R-loops [4, 13], it is possible that some AGS phenotypes arise from altered activity against R-loops. Indeed, cells with AGS alleles have increased R-loop accumulation [7].

Supplementary Material

Refer to Web version on PubMed Central for supplementary material.

Acknowledgments

We thank Duncan Smith for comments. Eli Rothenberg and Yandong Yin provided invaluable help with scanning and quantification of the alkaline gels. Beatrix Ueberheide provided assistance with protein alignments. Support from the National Institutes of Health R01CA146940 is acknowledged.

Abbreviations:

AGS Aicardi-Goutières Syndrome

DSB	double-strand break
HR	homologous recombination
Top1	topoisomerase 1
LOH	loss of heterozygosity
RER	ribonucleotide excision repair
dNTP	deoxynucleotide triphosphate
rNTP	ribonucleotide triphosphate
rNMP	ribonucleotide monophosphate

References

- [1]. Aicardi J, Goutieres F, A progressive familial encephalopathy in infancy with calcifications of the basal ganglia and chronic cerebrospinal fluid lymphocytosis, *Ann Neurol*, 15 (1984) 49–54. [PubMed: 6712192]
- [2]. Rice G, Patrick T, Parmar R, Taylor CF, Aeby A, Aicardi J, Artuch R, Montalto SA, Bacino CA, Barroso B, Baxter P, Benko WS, Bergmann C, Bertini E, Biancheri R, Blair EM, Blau N, Bonthron DT, Briggs T, Brueton LA, Brunner HG, Burke CJ, Carr IM, Carvalho DR, Chandler KE, Christen HJ, Corry PC, Cowan FM, Cox H, D'Arrigo S, Dean J, De Laet C, De Praeter C, Dery C, Ferrie CD, Flintoff K, Frints SG, Garcia-Cazorla A, Gener B, Goizet C, Goutieres F, Green AJ, Guet A, Hamel BC, Hayward BE, Heiberg A, Hennekam RC, Husson M, Jackson AP, Jayatunga R, Jiang YH, Kant SG, Kao A, King MD, Kingston HM, Klepper J, van der Knaap MS, Kornberg AJ, Kotzot D, Kratzer W, Lacombe D, Lagae L, Landrieu PG, Lanzi G, Leitch A, Lim MJ, Livingston JH, Lourenco CM, Lyall EG, Lynch SA, Lyons MJ, Marom D, McClure JP, McWilliam R, Melancon SB, Mewasingh LD, Moutard ML, Nischal KK, Ostergaard JR, Prendiville J, Rasmussen M, Rogers RC, Roland D, Rosser EM, Rostasy K, Roubertie A, Sanchis A, Schiffmann R, Scholl-Burgi S, Seal S, Shalev SA, Corcoles CS, Sinha GP, Soler D, Spiegel R, Stephenson JB, Tacke U, Tan TY, Till M, Tolmie JL, Tomlin P, Vagnarelli F, Valente EM, Van Coster RN, Van der Aa N, Vanderver A, Vles JS, Voit T, Wassmer E, Weschke B, Whiteford ML, Willemsen MA, Zankl A, Zuberi SM, Orcesi S, Fazzi E, Lebon P, Crow YJ, Clinical and molecular phenotype of Aicardi-Goutieres syndrome, *Am J Hum Genet*, 81 (2007) 713–725. [PubMed: 17846997]
- [3]. Crow YJ, Livingston JH, Aicardi-Goutieres syndrome: an important Mendelian mimic of congenital infection, *Dev Med Child Neurol*, 50 (2008) 410–416. [PubMed: 18422679]
- [4]. Cerritelli SM, Crouch RJ, Ribonuclease H: the enzymes in eukaryotes, *FEBS J*, 276 (2009) 1494–1505. [PubMed: 19228196]
- [5]. Hiller B, Achleitner M, Glage S, Naumann R, Behrendt R, Roers A, Mammalian RNase H2 removes ribonucleotides from DNA to maintain genome integrity, *J Exp Med*, 209 (2012) 1419–1426. [PubMed: 22802351]
- [6]. Nick McElhinny SA, Kumar D, Clark AB, Watt DL, Watts BE, Lundstrom EB, Johansson E, Chabes A, Kunkel TA, Genome instability due to ribonucleotide incorporation into DNA, *Nat Chem Biol*, 6 (2010) 774–781. [PubMed: 20729855]
- [7]. Lim YW, Sanz LA, Xu X, Hartono SR, Chedin F, Genome-wide DNA hypomethylation and RNA:DNA hybrid accumulation in Aicardi-Goutieres syndrome, *Elife*, 4 (2015).
- [8]. Crow YJ, Chase DS, Lowenstein Schmidt J, Szykiewicz M, Forte GM, Gornall HL, Oojageer A, Anderson B, Pizzino A, Helman G, Abdel-Hamid MS, Abdel-Salam GM, Ackroyd S, Aeby A, Agosta G, Albin C, Allon-Shalev S, Arellano M, Ariaudo G, Aswani V, Babul-Hirji R, Baildam EM, Bahi-Buisson N, Bailey KM, Barnerias C, Barth M, Battini R, Beresford MW, Bernard G, Bianchi M, Billette de Villemeur T, Blair EM, Bloom M, Burlina AB, Carpanelli ML, Carvalho

DR, Castro-Gago M, Cavallini A, Cereda C, Chandler KE, Chitayat DA, Collins AE, Sierra Corcoles C, Cordeiro NJ, Crichiutti G, Dabydeen L, Dale RC, D'Arrigo S, De Goede CG, De Laet C, De Waele LM, Denzler I, Desguerre I, Devriendt K, Di Rocco M, Fahey MC, Fazzi E, Ferrie CD, Figueiredo A, Gener B, Goizet C, Gowrinathan NR, Gowrishankar K, Hanrahan D, Isidor B, Kara B, Khan N, King MD, Kirk EP, Kumar R, Lagae L, Landrieu P, Lauffer H, Laugel V, La Piana R, Lim MJ, Lin JP, Linnankivi T, Mackay MT, Marom DR, Marques Lourenco C, McKee SA, Moroni I, Morton JE, Moutard ML, Murray K, Nabbout R, Nampoothiri S, Nunez-Enamorado N, Oades PJ, Olivier I, Ostergaard JR, Perez-Duenas B, Prendiville JS, Ramesh V, Rasmussen M, Regal L, Ricci F, Rio M, Rodriguez D, Roubertie A, Salvatici E, Segers KA, Sinha GP, Soler D, Spiegel R, Stodberg TI, Straussberg R, Swoboda KJ, Suri M, Tacke U, Tan TY, te Water Naude J, Wee Teik K, Thomas MM, Till M, Tonduti D, Valente EM, Van Coster RN, van der Knaap MS, Vassallo G, Vijzelaar R, Vogt J, Wallace GB, Wassmer E, Webb HJ, Whitehouse WP, Whitney RN, Zaki MS, Zuberi SM, Livingston JH, Rozenberg F, Lebon P, Vanderver A, Orcesi S, Rice GI, Characterization of human disease phenotypes associated with mutations in TREX1, RNASEH2A, RNASEH2B, RNASEH2C, SAMHD1, ADAR, and IFIH1, *Am J Med Genet A*, 167A (2015) 296–312. [PubMed: 25604658]

- [9]. Reijns MA, Rabe B, Rigby RE, Mill P, Astell KR, Lettice LA, Boyle S, Leitch A, Keighren M, Kilanowski F, Devenney PS, Sexton D, Grimes G, Holt IJ, Hill RE, Taylor MS, Lawson KA, Dorin JR, Jackson AP, Enzymatic removal of ribonucleotides from DNA is essential for mammalian genome integrity and development, *Cell*, 149 (2012) 1008–1022. [PubMed: 22579044]
- [10]. Kim N, Huang SN, Williams JS, Li YC, Clark AB, Cho JE, Kunkel TA, Pommier Y, Jinks-Robertson S, Mutagenic processing of ribonucleotides in DNA by yeast topoisomerase I, *Science*, 332 (2011) 1561–1564. [PubMed: 21700875]
- [11]. Potenski CJ, Niu H, Sung P, Klein HL, Avoidance of ribonucleotide-induced mutations by RNase H2 and Srs2-Exo1 mechanisms, *Nature*, 511 (2014) 251–254. [PubMed: 24896181]
- [12]. Aguilera A, Klein HL, Genetic control of intrachromosomal recombination in *Saccharomyces cerevisiae*. I. Isolation and genetic characterization of hyper-recombination mutations, *Genetics*, 119 (1988) 779–790. [PubMed: 3044923]
- [13]. Chon H, Sparks JL, Rychlik M, Nowotny M, Burgers PM, Crouch RJ, Cerritelli SM, RNase H2 roles in genome integrity revealed by unlinking its activities, *Nucleic Acids Res*, 41 (2013) 3130–3143. [PubMed: 23355612]
- [14]. Epshtein A, Potenski CJ, Klein HL, Increased Spontaneous Recombination in RNase H2-Deficient Cells Arises From Multiple Contiguous rNMPs and Not From Single rNMP Residues Incorporated by DNA Polymerase Epsilon, *Microb Cell*, 3 (2016) 248–254. [PubMed: 28203566]
- [15]. Li M, Li T, Mironova LI, Brill SJ, Epistasis analysis between homologous recombination genes in *Saccharomyces cerevisiae* identifies multiple repair pathways for Sgs1, Mus81-Mms4 and RNase H2, *Mutat Res*, 714 (2011) 33–43. [PubMed: 21741981]
- [16]. Crow YJ, Leitch A, Hayward BE, Garner A, Parmar R, Griffith E, Ali M, Semple C, Aicardi J, Babul-Hirji R, Baumann C, Baxter P, Bertini E, Chandler KE, Chitayat D, Cau D, Dery C, Fazzi E, Goizet C, King MD, Klepper J, Lacombe D, Lanzi G, Lyall H, Martinez-Frias ML, Mathieu M, McKeown C, Monier A, Oade Y, Quarrell OW, Rittey CD, Rogers RC, Sanchis A, Stephenson JB, Tacke U, Till M, Tolmie JL, Tomlin P, Voit T, Weschke B, Woods CG, Lebon P, Bonthron DT, Ponting CP, Jackson AP, Mutations in genes encoding ribonuclease H2 subunits cause Aicardi-Goutieres syndrome and mimic congenital viral brain infection, *Nat Genet*, 38 (2006) 910–916. [PubMed: 16845400]
- [17]. den Dunnen JT, Dalgleish R, Maglott DR, Hart RK, Greenblatt MS, McGowan-Jordan J, Roux AF, Smith T, Antonarakis SE, Taschner PE, HGVS Recommendations for the Description of Sequence Variants: 2016 Update, *Hum Mutat*, 37 (2016) 564–569. [PubMed: 26931183]
- [18]. Rohman MS, Koga Y, Takano K, Chon H, Crouch RJ, Kanaya S, Effect of the disease-causing mutations identified in human ribonuclease (RNase) H2 on the activities and stabilities of yeast RNase H2 and archaeal RNase HII, *FEBS J*, 275 (2008) 4836–4849. [PubMed: 18721139]
- [19]. Chon H, Vassilev A, DePamphilis ML, Zhao Y, Zhang J, Burgers PM, Crouch RJ, Cerritelli SM, Contributions of the two accessory subunits, RNASEH2B and RNASEH2C, to the activity and

- properties of the human RNase H2 complex, *Nucleic Acids Res*, 37 (2009) 96–110. [PubMed: 19015152]
- [20]. Figiel M, Chon H, Cerritelli SM, Cybulska M, Crouch RJ, Nowotny M, The structural and biochemical characterization of human RNase H2 complex reveals the molecular basis for substrate recognition and Aicardi-Goutieres syndrome defects, *J Biol Chem*, 286 (2011) 10540–10550. [PubMed: 21177858]
- [21]. Reijns MA, Bubeck D, Gibson LC, Graham SC, Baillie GS, Jones EY, Jackson AP, The structure of the human RNase H2 complex defines key interaction interfaces relevant to enzyme function and human disease, *J Biol Chem*, 286 (2011) 10530–10539. [PubMed: 21177854]
- [22]. Spell RM, Jinks-Robertson S, Determination of mitotic recombination rates by fluctuation analysis in *Saccharomyces cerevisiae*, *Methods Mol Biol*, 262 (2004) 3–12. [PubMed: 14769952]
- [23]. Lea DE, Coulson CA, The distribution of the numbers of mutants in bacterial populations, *J Genet*, 49 (1949) 264–285. [PubMed: 24536673]
- [24]. Roy A, Kucukural A, Zhang Y, I-TASSER: a unified platform for automated protein structure and function prediction, *Nat Protoc*, 5 (2010) 725–738. [PubMed: 20360767]
- [25]. Roy A, Yang J, Zhang Y, COFACTOR: an accurate comparative algorithm for structure-based protein function annotation, *Nucleic Acids Res*, 40 (2012) W471–477. [PubMed: 22570420]
- [26]. El Hage A, French SL, Beyer AL, Tollervey D, Loss of Topoisomerase I leads to R-loop-mediated transcriptional blocks during ribosomal RNA synthesis, *Genes & development*, 24 (2010) 1546–1558. [PubMed: 20634320]
- [27]. Lippert MJ, Kim N, Cho JE, Larson RP, Schoenly NE, O'Shea SH, Jinks-Robertson S, Role for topoisomerase I in transcription-associated mutagenesis in yeast, *Proc Natl Acad Sci U S A*, 108 (2011) 698–703. [PubMed: 21177427]
- [28]. Pokatayev V, Hasin N, Chon H, Cerritelli SM, Sakhuja K, Ward JM, Morris HD, Yan N, Crouch RJ, RNase H2 catalytic core Aicardi-Goutieres syndrome-related mutant invokes cGAS/STING innate immune-sensing pathway in mice, *J Exp Med*, 213 (2016) 329–336. [PubMed: 26880576]
- [29]. Nick McElhinny SA, Watts BE, Kumar D, Watt DL, Lundstrom EB, Burgers PM, Johansson E, Chabes A, Kunkel TA, Abundant ribonucleotide incorporation into DNA by yeast replicative polymerases, *Proc Natl Acad Sci U S A*, 107 (2010) 4949–4954. [PubMed: 20194773]
- [30]. Harding SM, Benci JL, Irianto J, Discher DE, Minn AJ, Greenberg RA, Mitotic progression following DNA damage enables pattern recognition within micronuclei, *Nature*, 548 (2017) 466–470. [PubMed: 28759889]
- [31]. Mackenzie KJ, Carroll P, Martin CA, Murina O, Fluteau A, Simpson DJ, Olova N, Sutcliffe H, Rainger JK, Leitch A, Osborn RT, Wheeler AP, Nowotny M, Gilbert N, Chandra T, Reijns MAM, Jackson AP, cGAS surveillance of micronuclei links genome instability to innate immunity, *Nature*, 548 (2017) 461–465. [PubMed: 28738408]
- [32]. Mackenzie KJ, Carroll P, Lettice L, Tarnauskaite Z, Reddy K, Dix F, Revuelta A, Abbondati E, Rigby RE, Rabe B, Kilanowski F, Grimes G, Fluteau A, Devenney PS, Hill RE, Reijns MA, Jackson AP, Ribonuclease H2 mutations induce a cGAS/STING-dependent innate immune response, *EMBO J*, 35 (2016) 831–844. [PubMed: 26903602]
- [33]. Kondo T, Kobayashi J, Saitoh T, Maruyama K, Ishii KJ, Barber GN, Komatsu K, Akira S, Kawai T, DNA damage sensor MRE11 recognizes cytosolic double-stranded DNA and induces type I interferon by regulating STING trafficking, *Proc Natl Acad Sci U S A*, 110 (2013) 2969–2974. [PubMed: 23388631]
- [34]. Huang SN, Williams JS, Arana ME, Kunkel TA, Pommier Y, Topoisomerase I-mediated cleavage at unrepaired ribonucleotides generates DNA double-strand breaks, *EMBO J*, 36 (2017) 361–373. [PubMed: 27932446]

Highlights

- AGS mutations in RNase H2 subunits can be modeled in yeast
- Some AGS alleles have no observable phenotype in yeast
- Other AGS alleles have strong negative impact on genome stability
- in vivo yeast phenotypes correlate with increased retention of rNMPs in DNA

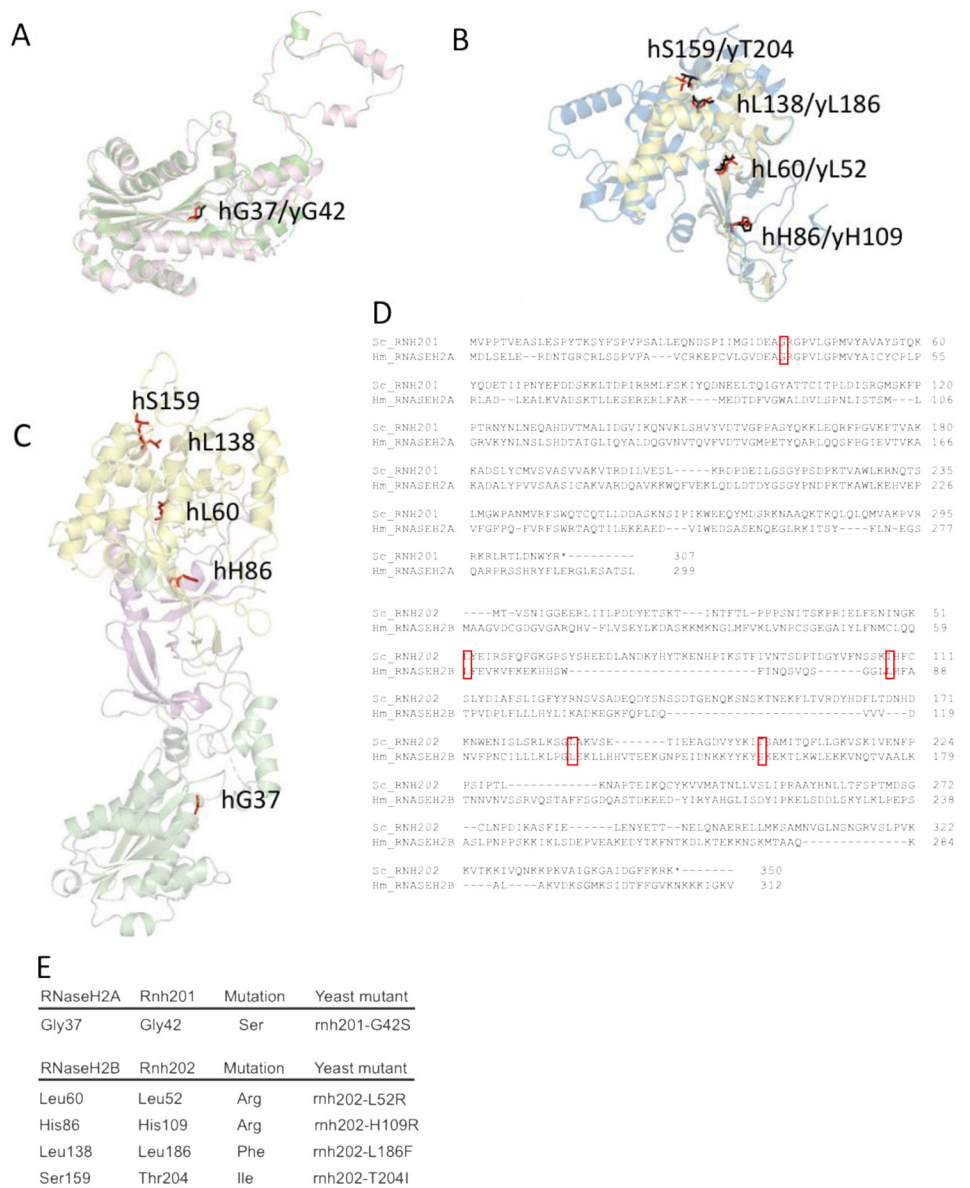


Figure 1. Conserved AGS-associated residues from yeast to humans. Homology models of yeast Rnh201 and Rnh202 were generated and aligned to structural models of human RNASEH2A and RNASEH2B, respectively. Conserved AGS-associated residues were identified on the aligned yeast homology structures. **A.** We chose one conserved residue in yRnh201 (magenta) / hRNASEH2A (green): yGly42(red) / hGly37(black). **B.** We chose four conserved residues in yRnh202(blue) / hRNASEH2B(yellow): 1.) yHis109/hHis86; 2.) yLeu52/hLeu60; 3.) yLeu186/hLeu138; 4.) yThr204/hSer159 (yeast residues in red, human residues in black). **C. Conserved residues identified are located in different parts of the enzyme complex.** The structure (PDB ID = 3PUFR) of the RNase H2 heterotrimeric complex consisting of RNASEH2A (green), RNASEH2B (yellow) and RNASEH2C (magenta) is shown with AGS-associated residues (red) that are conserved in yeast highlighted. **D. Alignment of yeast Rnh201 with human**

RNASEH2A and yeast Rnh202 with human RNASEH2B. The top panel shows the alignment of Rnh201 with RNASEH2A using Clustal Omega. The lower panel shows the alignment of Rnh202 with RNASEH2B using Clustal Omega. The red boxes indicate the position of the human AGS mutations shown in panels A, B and E and their alignment with the cognate yeast residue. **E. Mutations of the RNase H2 complex found in AGS patients are reconstructed in yeast strains.** Yeast cells with the appropriate amino acid change that reflects AGS mutations were constructed.

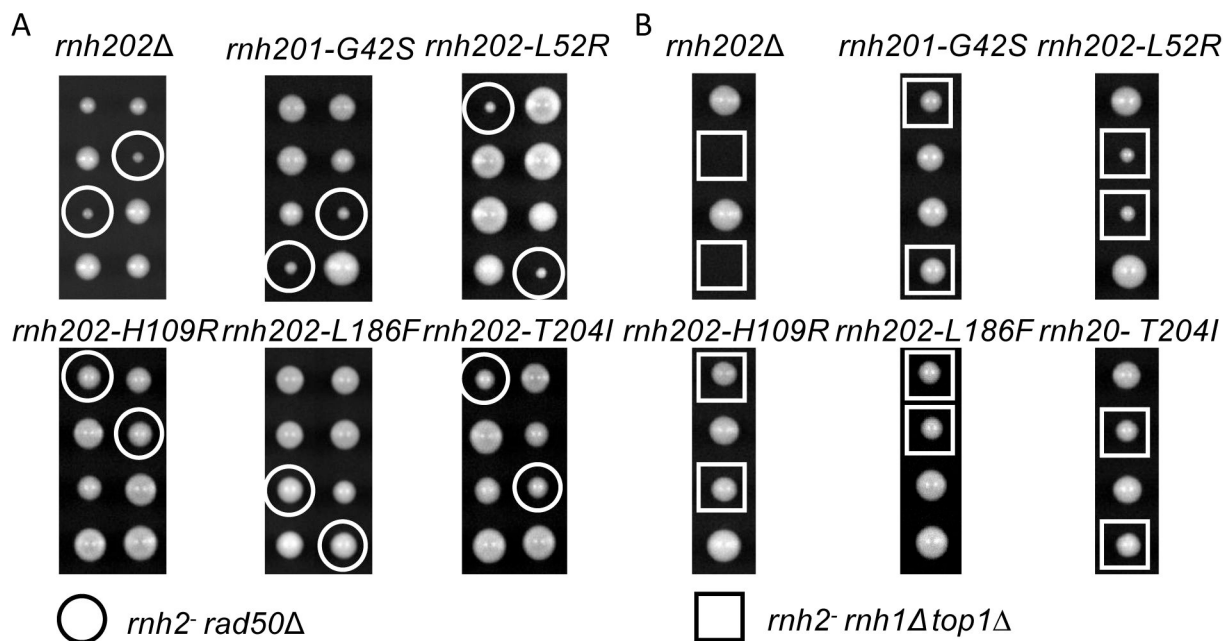


Figure 2. Synthetic genetic interactions.

A. Synthetic gene interactions with *rad50* . The yeast AGS mutants were crossed to a *rad50* strain, sporulated and the resultant tetrads were dissecting in an ordered array. Genotypes of the spores were determined. Double *rad50* *rnaseH2*-AGS mutants are circled in white. **B. Synthetic gene interactions with *rnh1 top1*** . The yeast AGS mutants were crossed to a *rnh1 top1* strain, sporulated and the resultant tetrads were dissecting in an ordered array. Genotypes of the spores were determined. Triple *rnh1 top1* *rnaseH2*-AGS mutants are indicated in white squares.

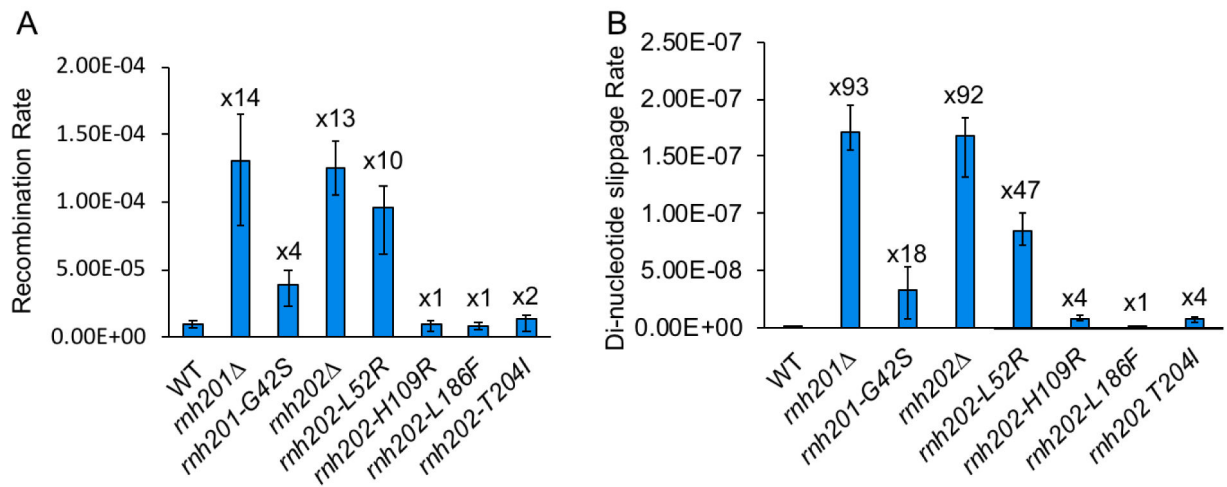


Figure 3. Genome instability assays

A. Recombination rates of rnh2-AGS mutants. A recombination reporter consisting of direct LEU2 repeats flanking a URA3 marker was used for fluctuation analysis to determine gene conversion rates. Error bars represent the standard deviation from 3 independent experiments, and fold increase from wild type level is reported above the bars. **B.**

Dinucleotide slippage mutation rate of rnh2-AGS mutants. Rates of dinucleotide slippage were determined using a reporter containing an (AG)₄ tandem repeat embedded in the *LYS2* gene. Fluctuation analysis was used to determine rates, and error bars represent the standard deviation from 3 independent experiments, and fold increase from wild type level is reported above the bars.

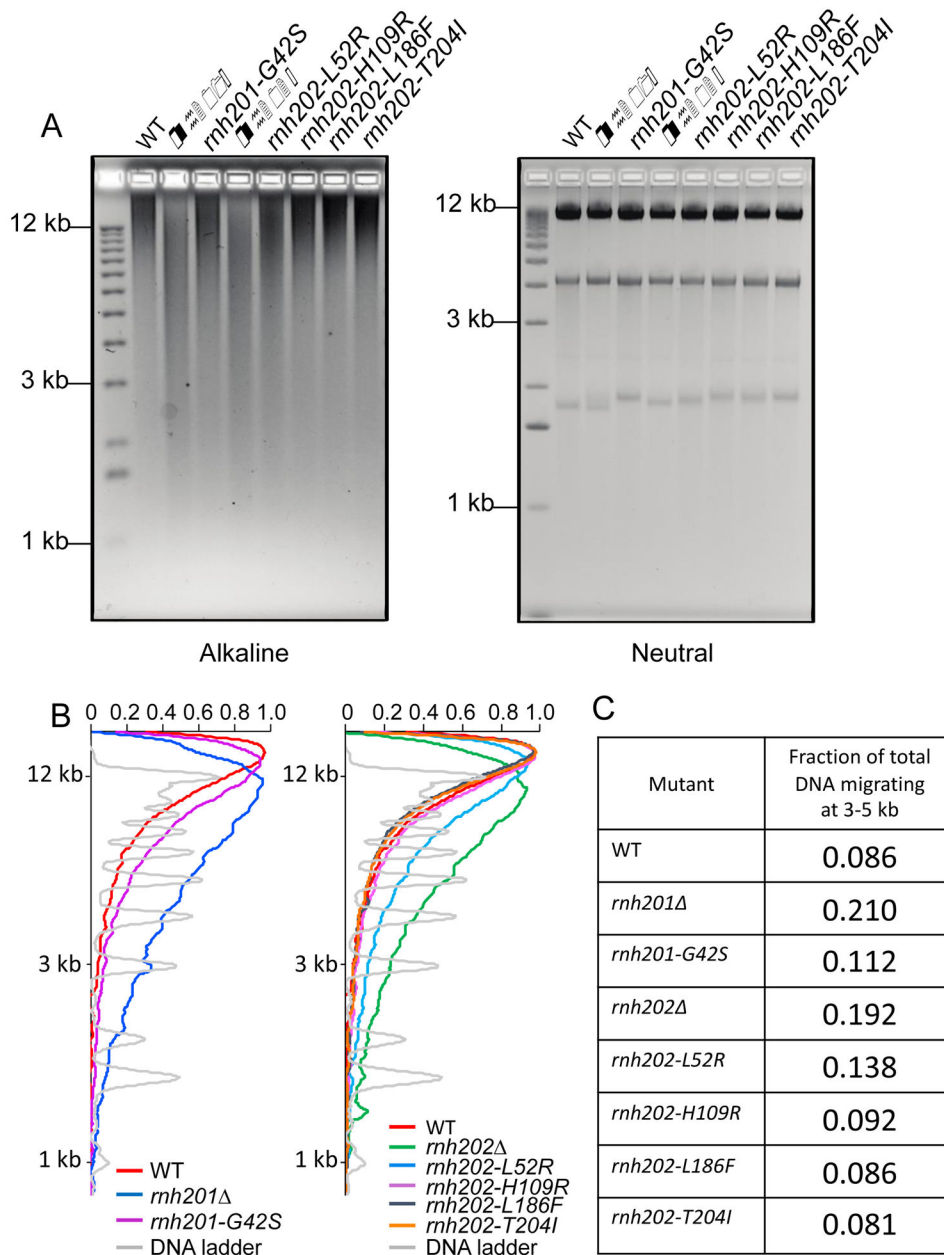


Figure 4. Assessment of ribonucleotides in genomic DNA

A. Alkaline gel analysis of genomic DNA. Genomic DNA was isolated from the indicated strains, treated with 0.3 N KOH for 2 hours at 55°C and run on 1% agarose gel in alkaline buffer. Gels were neutralized and stained with ethidium bromide. For the neutral gel, untreated DNA was run on 1% agarose gel in 1XTBE and stained with ethidium bromide. **B. Scans of alkaline gel lanes.** Densitometry tracings using MatLab of lanes of the alkaline gel in (A), presenting the RNH201 alleles and the RNH202 alleles separately. **C. Fraction of total DNA fragments migrating at 3-5 kb in each lane.** The fraction of fragments migrating at 3-5 kb in each sample on the alkaline gel was calculated from the MatLab tracings. Genomic DNA from the *rnh201-G42S* and *rnh202-L52R* strains show an increase

in this fraction compared to wildtype but in both cases it is less than the respective null strain. The X-axis has arbitrary labels, normalizing the maximum of each peak to 1.

Author Manuscript

Author Manuscript

Author Manuscript

Author Manuscript